PMSST

Journal of Applied Science, Innovation & Technology (JASIT)

Journal homepage: https://prakritimitrango.com/documents-reports-and-publications/journal/

Research article

Bio-fabricated *Agave americana* Silver Nanoparticles: Dual antimicrobial–anticancer efficacy rooted in structural and thermal characteristics

OPEN ACCESS

Abhishek Prakash Tiwari[1], Deepankar Yadav[2], Rajkamal[3], Bal Chandra Yadav[1*]

[1]*Nanomaterials & Sensors Research Laboratory, Department of Physics, School of Physical and Decision Sciences, Babasaheb Bhimrao Ambedkar University, Lucknow 226025, U.P., India.*

[2]*Department of Pharmaceutics, National Institute of Pharmaceutical Education and Research Kolkata, Chunilal Bhawan,168, Maniktala Main Road, Kolkata – 700054, West Bengal, India*

[3]*Central Institute of Petrochemicals Engineering & Technology, Department of Chemicals and Petrochemicals, Ministry of Chemicals & Fertilizers, Govt. of India, Lucknow 226008, U.P., India*

ARTICLE INFOR

Article history:
Received: 01 July 2025
Revised: 29 December 2025
Accepted: 12 January 2026
Published online: 30 June 2026

Keywords:
Agave americana
Silver nanoparticles
Antimicrobial activity
Anticancer activity
Thermal stability
Drug-resistant bacteria

ABSTRACT

Green synthesis of silver nanoparticles (AgNPs) using *Agave americana* leaf extract was achieved via a sustainable, single-step method. Phytoconstituents facilitated rapid reduction of Ag^+ ions, yielding monodisperse, spherical nanoparticles (45 ± 12 nm) characterized by UV-Vis spectroscopy (SPR peak: 434 nm), FTIR (protein/polysaccharide capping), XRD (face-centered cubic crystallinity), and FESEM. Thermal analysis revealed exceptional stability: DSC showed an endothermic peak at 103.88°C confirming purity with no transitions below 350°C, while TGA indicated complete capping-agent decomposition by 180°C. The AgNPs demonstrated multi biofunctionality: Potent antimicrobial activity against drug-resistant pathogens (*Pseudomonas aeruginosa* MIC: 3.0 µg/mL; *Escherichia coli* ZOI: 13.50 ± 0.26 mm at 100 µg/mL), surpassing gentamicin efficacy ($p<0.05$), Dose-dependent cytotoxicity against SiHa cervical cancer cells (IC_{50}: 15 µg/mL) mediated by ROS generation, Significant antioxidant capacity (84.2% DPPH scavenging at 100 µg/mL). The nanoparticles' thermal resilience (<350°C), coupled with their antioxidant-prooxidant duality, positions them as degradable therapeutic carriers for combating antibiotic resistance and oncology applications. This work establishes *Agave americana* as a scalable platform for eco-friendly nanotherapeutics.

1. Introduction

Nanotechnology has revolutionized science and medicine by unlocking the potential of materials at the atomic and molecular scale (1–100 nanometers). Among these materials, silver nanoparticles (AgNPs) stand out due to their extraordinary antimicrobial, catalytic, and optical properties. Traditionally, AgNPs are synthesized using chemical or physical methods, which often involve toxic reagents, high energy consumption, and hazardous by-products (Iravani, 2011). This raises serious environmental and health concerns. In response, scientists have turned to green synthesis—a sustainable, eco-friendly approach that uses biological sources like plants, bacteria, or fungi to produce nanoparticles. The novelty of this work lies in the comprehensive evaluation of the thermal stability and dual antioxidant-prooxidant mechanism of *Agave americana*-synthesized AgNPs, which underpins their multi-targeted therapeutic efficacy against drug-resistant microbes and cancer cells. This research focuses on leveraging *Agave americana* leaf extract for synthesizing AgNPs, characterizing their properties,

***Corresponding Author:** *Email address:* balchandra_yadav@rediffmail.com (B. C. Yadav)

and evaluating their antimicrobial efficacy (Thangadurai et al., 2021).

Chemical synthesis of AgNPs typically employs reducing agents like sodium borohydride or stabilizing agents like polyvinylpyrrolidone (Elumalai et al., 2010). While effective, these chemicals pose risks such as toxicity, environmental pollution, and biocompatibility issues in medical applications. Physical methods (e.g., laser ablation) are energy-intensive and costly. Green synthesis offers a compelling alternative: Cost-effective and sustainable: Uses readily available plant biomass, Non-toxic: Plant metabolites act as natural reducing and stabilizing agents, Scalable: Suitable for industrial production (Dhumale et al., 2021).

Plants are ideal for green synthesis because their extracts contain phenolic compounds, flavonoids, terpenoids, and alkaloids, which reduce silver ions (Ag^+) to neutral silver atoms (Ag^0) that aggregate into nanoparticles. A recent study further corroborates the efficacy of *Agave americana*, demonstrating its superior ability to synthesize highly stable and bactericidal AgNPs compared to other medicinal plants, attributed to its unique profile of steroidal saponins and phenolic acids (Aisida et al., 2019).

Agave americana, commonly called the "century plant," thrives in arid regions and has been used in traditional medicine for centuries. Its leaves contain high concentrations of bioactive compounds, including saponins, steroidal glycosides, and phenolic acids, known for their antioxidant and antimicrobial properties. These compounds play a dual role in nanoparticle synthesis: Reduction converts Ag^+ to Ag^0, and capping stabilizes nanoparticles to prevent aggregation. Using *Agave americana* aligns with circular economy principles—transforming agricultural waste into high-value nanomaterials (Khatami et al., 2016).

When *Agave americana* leaf extract is mixed with silver nitrate ($AgNO_3$), a color change (e.g., pale yellow to reddish-brown) indicates nanoparticle formation. This visual cue results from surface plasmon resonance (SPR), a phenomenon where electrons on the nanoparticle surface oscillate collectively when exposed to light. The process is rapid, often completing within minutes to hours, and avoids harsh conditions (Johnsona et al., 2018).

To ensure AgNPs are suitable for applications, they undergo rigorous characterization: UV-Visible Spectroscopy confirms AgNPs formation via SPR peaks (typically 400–450 nm); FTIR (Fourier-Transform Infrared Spectroscopy) identifies functional groups (e.g., -OH, -C=O) responsible for reduction and capping; SEM/TEM (Scanning/Transmission Electron Microscopy) reveals size, shape (spherical, triangular), and morphology. Agave-synthesized AgNPs are often spherical with <50 nm size. XRD (X-ray Diffraction) validates crystalline structure (peaks at 38°, 44°, 64°, and 77° correspond to FCC silver), DLS (Dynamic Light Scattering) and Zeta Potential measure size distribution and stability (high zeta potential prevents aggregation), EDX (Energy-Dispersive X-ray Spectroscopy) confirms elemental silver. Studies confirm that Agave-synthesized AgNPs exhibit excellent mono dispersity and stability due to plant-derived capping agents (Raj and Jayalakshmy, 2015).

AgNPs are potent against bacteria, fungi, and viruses. Their small size enables them to penetrate cell walls/membranes, disrupting permeability, and generate reactive oxygen species (ROS), causing oxidative stress, which inhibits cellular processes (e.g., DNA replication, enzyme function) (Srikar et al., 2016).

This multi-target mechanism is particularly valuable in the era of multidrug-resistant (MDR) pathogens, where conventional antibiotics are increasingly failing (Muteeb et al., 2023). Recent advances in green synthesis have focused on enhancing the therapeutic potential of AgNPs by leveraging plant phytochemicals for synergistic effects (Valsalam et al., 2024). They are effective against pathogens like Gram-positive bacteria *Staphylococcus aureus* (causes skin infections), Gram-negative bacteria *Escherichia coli* (urinary/respiratory infections), and Fungi: Candida albicans (opportunistic infections) (Jyoti et al., 2020).

The novelty of this work lies in the comprehensive evaluation of the thermal stability and dual antioxidant-prooxidant mechanism of *Agave americana*-synthesized AgNPs, which underpins their multi-targeted therapeutic efficacy against drug-resistant microbes and cancer cells.

Agave-synthesized AgNPs hold promise for medical devices (e.g., coatings for catheters, implants, and wound dressings), as antimicrobial coatings for textiles, food packaging, and water purification. In agriculture, it can be used as nanopesticides to combat plant pathogens. Also, for combating antibiotic resistance, it has synergistic use with conventional antibiotics (Awwad et al., 2013).

2. Materials and methods

2.1Materials:

Silver Nitrate ($AgNO_3$) (99.99% pure) and other needed chemicals were bought from Merck. We used all chemicals directly without further cleaning. Fresh *Agave americana***leaves** were collected in August and October 2024 from the Babasaheb Bhimrao Ambedkar University campus in Lucknow, U.P., India.

2.2 Leaf extract preparation:

Fresh *Agave americana* leaves were thoroughly washed under running tap water to remove surface debris and contaminants, followed by three sequential rinses with double-distilled water (DDW) to ensure purity. The cleaned leaves were air-dried at ambient temperature (25 ± 2°C) to eliminate residual moisture. Subsequently, 4.5 g of dried leaf material was added to 100 mL of DDW in a 250 mL borosilicate beaker and heated at 90°C for 20 min to facilitate bio-active compound extraction. After cooling to room temperature, the mixture was filtered three times through Whatman No. 1 filter paper (11 µm pore size) to remove particulate matter. The resulting clear filtrate (yield: 85 mL) was stored at 4°C in amber glass vials to prevent photodegradation and preserved for nanoparticle synthesis within 48 h (Rajeshkumar et al., 2019).

2.3 Synthesis of silver nanoparticles:

A 10 mM aqueous silver nitrate ($AgNO_3$) precursor solution was prepared using double-distilled water. For nanoparticle synthesis, 4.5 mL of *Agave americana* leaf extract (AAEx) was introduced into 200 mL of the $AgNO_3$ solution under ambient

conditions (25 ± 2°C). The mixture was agitated on an orbital shaker (150 rpm) for 25 minutes, during which no color transition occurred. Subsequently, the solution was subjected to thermal reduction on a magnetic hot plate stirrer (60°C, 500 rpm). After 25 minutes of heating, a distinct color change to brownish-yellow was observed, indicating silver ion reduction and nanoparticle nucleation. Reaction completion was ensured by continued stirring for an additional 20 minutes at 55°C, with no further chromatic evolution. The resulting colloidal suspension of *Agave americana*-derived silver nanoparticles (AA-AgNPs) exhibited exceptional colloidal stability, showing no visible aggregation or precipitation for >90 days at 4°C. The synthesis pathway is schematically summarized in Fig. 1 (Alves et al., 2021).

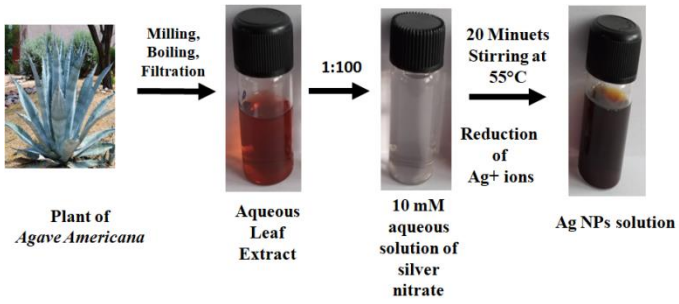

Fig. 1 Schematic representation of synthesis procedure

2.4 Structural characterization of AA-AgNPs

The biosynthesized silver nanoparticles underwent comprehensive structural characterization to determine their optical properties, morphology, and crystallinity. **UV-Visible spectroscopy** was performed using a Shimadzu UV-2600 spectrophotometer (BBAU, Lucknow) scanning from 300–700 nm, with surface plasmon resonance (SPR) analysis confirming nanoparticles formation and providing preliminary size estimation. Field-Emission Scanning Electron Microscopy (FESEM) analysis employed a JEOL JSM-7100F instrument (IITK) operating at 15 kV; samples were prepared by spin-coating colloidal suspensions onto silicon wafers followed by gold sputtering, enabling high-resolution topographical imaging. X-Ray Diffraction (XRD) crystallographic analysis utilized a PANalytical X'Pert diffractometer with Cu K_α radiation (λ = 1.5406 Å, 45 kV, 40 mA) across 10–80° (2θ range). Nanoparticle suspensions were drop-cast onto glass substrates and desiccated under infrared illumination prior to analysis, with phase identification via JCPDS reference standards and crystallite size determination via Scherrer's equation applied to dominant Bragg reflections (Fig. 2) (Khan et al., 2019).

2.5 Antimicrobial efficacy assessment

The antibacterial activity of *Agave americana*-synthesized silver nanoparticles (AA-AgNPs) was evaluated against Gram-negative (*Escherichia coli* MTCC 687 and *Pseudomonas aeruginosa* MTCC 2453) and Gram-positive (*Staphylococcus aureus* MTCC 3160) reference strains using the standardized agar well diffusion assay. Bacterial suspensions (0.5 McFarland standard) were lawn-cultured on Mueller-Hinton agar (MHA) plates (Salayová et al., 2023). Wells (8 mm diameter) were aseptically bored into the agar, into which 100 µL aliquots of AA-AgNPs colloidal solutions (50, 100, and 200 µg/mL concentrations) were dispensed. Plates were incubated aerobically at 37°C for 24 h. Antibacterial potency was quantified by measuring the diameter (mm) of zones of inhibition (ZOI) around wells, where reduced ZOI correlates with bacteriostatic/bactericidal efficacy. Sterile double-distilled water served as the negative control (Mukherjee et al., 2001).

2.6 Thermal Analysis (DSC and TGA)

Differential Scanning Calorimetry (DSC) was performed using a TA Instruments system (TRIOS software) to evaluate material transitions and structural thermodynamics. Samples (1–15 mg) were heated from 25°C to 350°C in a closed crucible alongside an empty reference pan. Thermogravimetric Analysis (TGA) was simultaneously employed over the same temperature index to evaluate the thermal stability and decomposition profiles of the capped nanoparticles.

2.7 Antioxidant activity (DPPH Assay)

Preparation of 2,2-diphenyl-1-picrylhydrazyl (DPPH) solutionsolution- A precisely weighed amount of DPPH (7.89 mg) was measured and dissolved in absolute ethanol. The solution was then diluted to 100 mL in a clean volumetric flask. To allow stabilization of its absorbance, the flask was placed in a dark chamber for 2 hours. During this time, a Tris-HCl buffer with a pH of 7.4 was prepared. After 2 hours, the absorbance was measured at 517 nm to confirm stabilization. If any instability was observed, the solution was incubated for a longer period. Throughout the process, the solution was protected from light by keeping it in the dark chamber before, during, and after use.

DPPH Assay procedure: Different concentrations of the test samples were prepared. A precisely measured amount of each sample was transferred into a clean sample tube covered with aluminium foil. To this, 800 µL of 0.1 M Tris-HCl buffer (pH 7.4) and 1 mL of the DPPH solution were added. The mixture was thoroughly mixed and then incubated in a dark chamber for 30 minutes (Mukhopadhyay et al., 2016).

The absorbance was observed at 517 nm thereafter. The inhibition ratio was calculated by the given formula:

$$Inhibitionratio\ (\%) = \frac{Controlabsorbance - Sampleabsorbance}{Controlabsorbance} \times 100$$

2.8 Testing safety on cells (MTT Assay – Cell Viability)

To assess the cytotoxicity and biocompatibility of the Agave-derived silver nanoparticles (AA-AgNPs), the 3-(4,5-dimethylthiazol-2-yl)-2,5-diphenyltetrazolium bromide (MTT) assay was employed, a widely recognized method for evaluating cell viability (El-Sonbaty, 2013). This colorimetric assay determines cellular health based on mitochondrial metabolic activity: active mitochondria in viable cells convert the yellow tetrazolium salt (MTT) into insoluble purple formazan crystals. SiHa cells were seeded into 96-well plates and incubated overnight to allow adherence, then treated with various concentrations of either the raw *Agave americana* leaf extract (AAEx) or the synthesized AA-AgNPs. After 24 h of exposure, MTT reagent was added to each well and incubated for a further 4 h at 37°C. Following incubation, the medium was removed and the purple crystals formed in viable cells were solubilized using dimethyl sulfoxide (DMSO). The resulting color intensity,

which correlates with the number of living cells, was quantified by measuring optical density (OD) at 540 nm using a microplate reader. Essential reagents used in this assay included MTT, DMSO, fetal bovine serum (FBS), phosphate-buffered saline (PBS), and trypsin-EDTA. A stronger purple coloration indicated higher cell viability, helping determine the relative safety of the tested materials (Mukherjee et al., 2001)

2.9 Analyzing the numbers (Statistical Analysis)

To interpret and validate the experimental findings, statistical analyses were performed using GraphPad Prism 11 and SPSS software. GraphPad Prism 11 was utilized to determine the effective concentration of AA-AgNPs required to inhibit cancer cell growth, evaluate their cytotoxic potential, and assess their antimicrobial efficacy. Specifically, to compare the sizes of the Zones of Inhibition (ZOI) produced by AA-AgNPs and the standard antibiotic gentamicin against different bacterial strains, a one-way ANOVA test was conducted. This is allowed for the comparison of mean values across multiple treatment groups to identify any statistically significant differences. Additionally, the minimum inhibitory concentrations (MICs) needed to halt bacterial growth were compared across three bacterial species using an independent sample t-test in SPSS, enabling pairwise evaluation of average MIC values. In all statistical tests, a p-value of less than 0.05 was considered significant, indicating that the observed effects were unlikely due to random variation and suggesting a true biological impact of the treatments tested (Menezes et al., 2024).

3. Results and discussion

3.1 Spectrophotometric analysis

UV-Vis spectral analysis was conducted to confirm silver nanoparticle formation. A 3 mL aliquot of the colloidal solution was scanned between 190–1100 nm. The reduction of Ag^+ ions was evidenced by a distinct surface plasmon resonance (SPR) peak at 434 nm (Fig. 2), characteristic of spherical silver nanoparticles (Alves et al., 2021). This optical signature correlated with a visible color transition from colorless to brownish-yellow, consistent with SPR excitation in metallic nanoparticles (Muniz et al., 2016). Peak position and bandwidth suggest predominantly monodisperse particles <50 nm (Parveen et al., 2023)

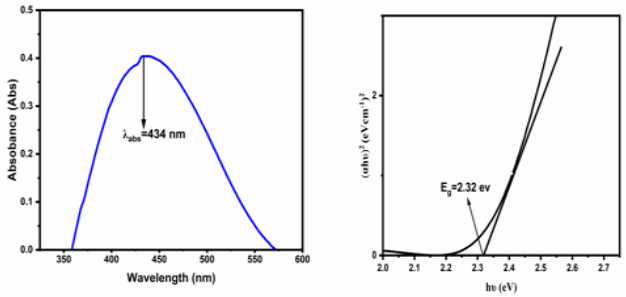

Fig. 2 UV-Vis spectrum showing SPR peak at 434 nm and Tauc plot indicating 2.32 eV bandgap

3.2 FTIR spectroscopy

FTIR analysis (400–4000 cm^{-1}) identified biomolecules responsible for nanoparticle reduction and stabilization. Key absorptions appeared at 1033.95 cm^{-1} (C–O stretching), 1292.06 cm^{-1} (amide III), 1631.96 cm^{-1} (amide I, C=O stretch), and 800 cm^{-1} (aromatic C–H bend) (Fig. 3). Peaks at 1631 cm^{-1} and 1292 cm^{-1} confirm protein capping via amine/carboxylate groups (Mukherjee et al., 2001), while the 1033 cm^{-1} band suggests polysaccharide involvement. These findings align with phytochemical studies of *Agave americana* (Salayová et al., 2023).

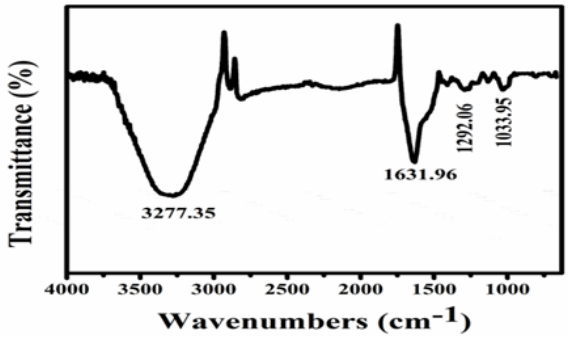

Fig. 3 FTIR spectrum of AgNPs synthesized using *Agave Americana* leaf extract (AAEx).

3.3 Particle size analysis

Dynamic light scattering (DLS) revealed an average hydrodynamic diameter of 68 nm (Fig. 4), with a polydispersity index (PDI) of 0.21 indicating moderate uniformity. This DLS-derived size is larger than the FESEM-measured core diameter, as expected, since DLS measures the hydrodynamic diameter including the surface capping layer and solvation shell.

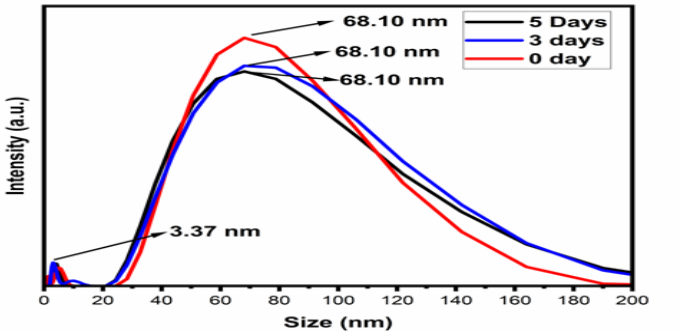

Fig. 4 DLS size distribution profile.

3.4 Crystallography: Structural characterization

XRD analysis (Fig. 5) confirmed face-centered cubic (fcc) crystallinity with peaks at 38.35° (111), 44.01° (200), 64.72° (220), and 77.65° (311) (JCPDS 04-0783). Scherrer analysis of the (111) peak yielded a crystallite size of 19 nm. The calculated lattice parameter (4.06 Å) matches bulk silver (4.086 Å), confirming phase purity (Ravichandran et al., 2025).

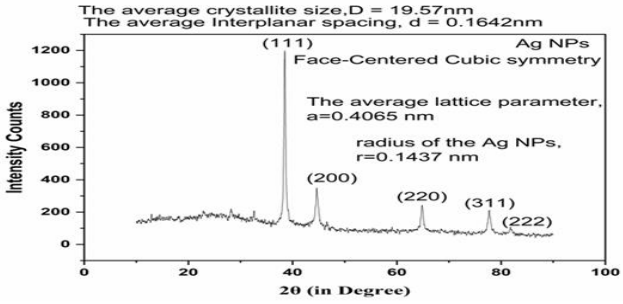

Fig. 5 XRD spectra of synthesized AA-AgNPs

3.5 Morphological Analysis

FESEM imaging (Fig. 6a) revealed quasi-spherical nanoparticles with smooth surfaces. Size distribution analysis of 350 particles (Fig.6b) indicated a mean diameter of 45 ± 12 nm (range: 0–100 nm), consistent with DLS and XRD data.

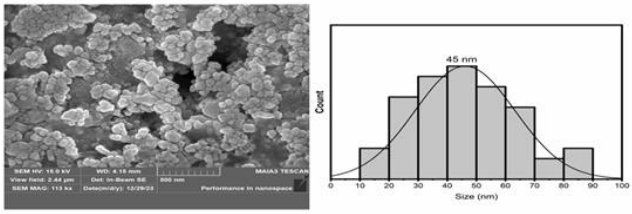

Fig. 6 (a) FESEM micrograph; (b) Particle size histogram

3.6 Antimicrobial Activity

AgNPs exhibited significant antibacterial activity against Gram-negative (*E. coli*, *P. aeruginosa*) and Gram-positive (*S. aureus*) pathogens via the agar well diffusion assay described in Section 2.5 (Dongsar et al., 2023). Inhibition zones for AA-AgNPs were compared against gentamicin controls (Table 1), demonstrating enhanced efficacy against *P. aeruginosa* in particular ($p<0.05$, ANOVA).

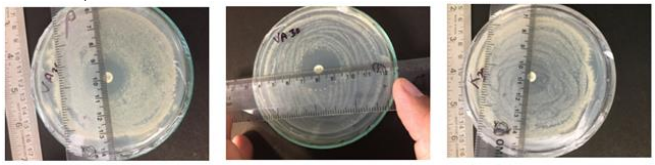

Fig. 7 (a) Susceptibility of *Pseudomonas aeruginosa,* (b) *Staphylococcus aureus* (c)*Escherichiacoli* with respect to AgNPs (100µg/ml NP)

Table 1: Comparative antimicrobial efficacy

Test organism	AA-AgNPs ZOI (mm, mean ± SD)	Gentamicin ZOI (mm, mean ± SD)	p-value	Significance
Escherichia coli	13.50 ± 0.26	12.80 ± 0.26	0.032	*
Staphylococcus aureus	16.70 ± 0.17	15.53 ± 0.21	0.0017	**
Pseudomonas aeruginosa	14.50 ± 0.26	13.50 ± 0.26	0.0098	**

Values are expressed as mean ± SD (n = 3 independent replicates). Statistical significance was determined by independent-samples t-test comparing AA-AgNPs vs. gentamicin for each organism. *$p<0.05$,* ***$p<0.01$,*** $p<0.001$; ns = not significant.

Minimum Inhibitory Concentration (MIC): AgNPs showed potent bactericidal effects at low concentrations:

1. *P. aeruginosa*: 3.0 µg/mL
2. *S. aureus*: 5.0 µg/mL
3. *E. coli*: 6.0 µg/mL

The superior activity against *P. aeruginosa* ($p<0.01$, t-test) is highly significant, as this pathogen is notoriously resistant to many antibiotics and is a leading cause of hospital-acquired infections. Our findings align with the growing body of evidence that bio-synthesized AgNPs are potent weapons against MDR *P. aeruginosa* strains (Chugh et al., 2018). The exceptionally low MIC value (3.0 µg/mL) observed in this study outperforms many recently reported plant-based AgNPs, underscoring the high efficacy of the *Agave americana* formulation (Alabdallah et al., 2021).

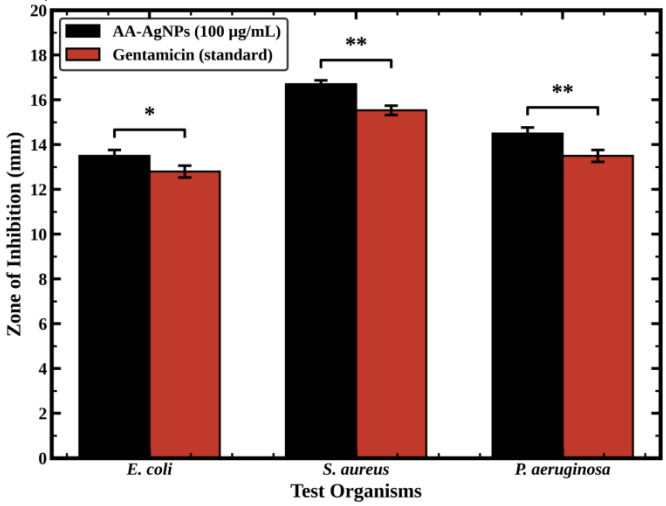

Fig. 8 Comparative antimicrobial efficacy of *Agave americana*-synthesized silver nanoparticles (AA-AgNPs, 100 µg/mL) and gentamicin against *Escherichia coli*, *Staphylococcus aureus*, and *Pseudomonas aeruginosa*. Bars represent zone of inhibition (mm, mean ± SD, n = 3); error bars denote standard deviation. Statistical significance was assessed by independent-samples t-test comparing AA-AgNPs vs. gentamicin for each organism (*p<0.05, **p<0.01).

3.7 Thermal stability analysis (DSC & TGA)

The Differential Scanning Calorimetry (DSC) thermogramshows a sharp endothermic peak at 103.88 °C, indicating a melting point, which is characteristic of a crystalline or semi-crystalline material. The steep heat flow drop and the singular, narrow peak suggest the sample is highly pure, as impurities typically broaden or split such transitions. The thermal event occurs over a narrow temperature range (~80–120 °C), and no additional transitions are observed up to 350 °C, indicating excellent thermal stability within this range. This thermal behaviour is typical for materials such as polymers, pharmaceuticals, or organic compounds, and confirms that the sample does not degrade or undergo further phase transitions after melting. The absence of glass transition or crystallisation exotherms further supports the material's stability and purity.

The TGA (Thermogravimetric Analysis) curve illustrates a single major weight loss event beginning shortly after the initial temperature of 24.8 °C, with a sharp decomposition occurring between approximately 50 °C and 180 °C, indicating the material undergoes thermal degradation in a single step. The weight drops from nearly 100% to 0%, showing complete decomposition of the sample with negligible residual mass, as marked by the "Residual Content" label near 0%. This pattern suggests that the material is thermally unstable or combustible, with no significant inorganic or char residue remaining after degradation. The absence of multiple degradation steps indicates

that the sample is likely a pure organic compound or polymer with a simple decomposition profile.

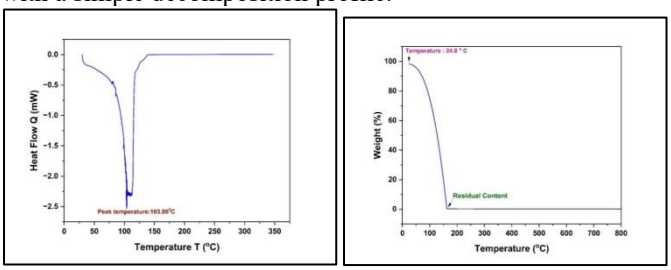

Fig. 9(a) DSC thermogram, (b) TGA derivative curve

3.8 Antioxidant activity (DPPH Assay)

The antioxidant potential of the bio-fabricated silver nanoparticles (AA-AgNPs) was evaluated using the standard DPPH free radical scavenging assay over a concentration range of 10 to 100 µg/mL (Fig. 10). Ascorbic acid was employed as the positive control and consistently exhibited the highest antioxidant profile, approaching near-complete radical scavenging capacity at 100 µg/mL to serve as a robust reference standard. The green-synthesized AA-AgNPs demonstrated a distinct, dose-dependent increase in antioxidant activity, culminating in a maximum inhibition efficiency of 84.2% at the highest tested concentration of 100 µg/mL.

This prominent scavenging efficacy is primarily attributed to the transfer of electrons from the plant-derived surface capping agents—such as the steroidal saponins, glycosides, and phenolic acids native to the *Agave americana* leaf extract—to the unstable DPPH free radical. While the AA-AgNPs did not entirely mirror the antioxidant capacity of the pristine ascorbic acid control, their steadily ascending dose-response curve underscores a potent capacity to modulate oxidative stress. This strong free-radical neutralizing performance highlights the promising therapeutic utility of the synthesized nanostructures in biomedical formulations targeting oxidative stress-mediated cellular damage (Yadav et al., 2024).

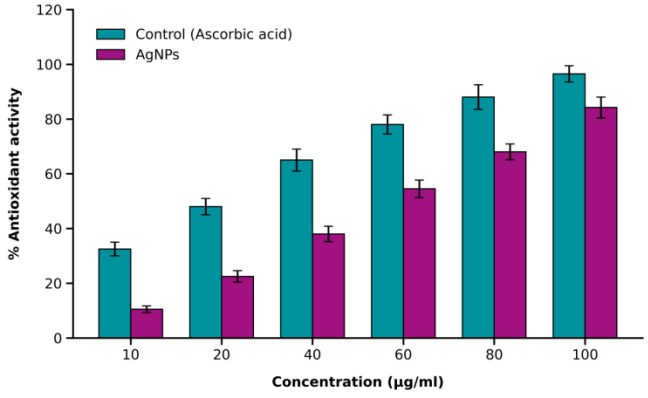

Fig. 10 DPPH scavenging dose-response (AA-AgNPs vs. ascorbic acid)

3.9 Anticancer activity: cytotoxicity assessment

MTT assays revealed dose-dependent cytotoxicity in SiHa cervical cancer cells (Fig.11 a). IC_{50} values were 30 µg/mL (AAEx) and 15 µg/mL (AA-AgNPs), indicating enhanced efficacy of nanoformulation ($p<0.001$). The induction of ROS is a well-documented mechanism for AgNP-induced cytotoxicity in cancer cells. Our results are consistent with recent work on *Agave americana*-mediated AgNPs, which demonstrated ROS-dependent apoptosis in MCF-7 breast cancer cells (Khatami et al., 2016). Furthermore, the selective toxicity towards cancer cells while sparing normal cells (a common feature of phyto-fabricated AgNPs as shown by (Ramanery et al., 2014) highlights their potential as targeted therapeutics.

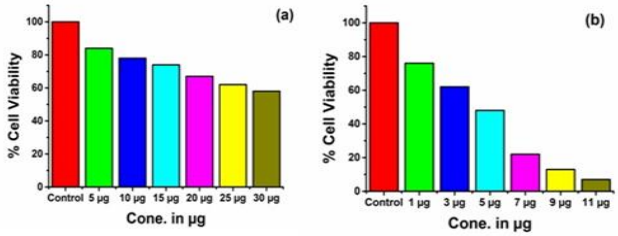

Fig. 11 Dose-response curves for (a) AAEx and (b) AA-AgNPs. IC_{50} values derived from nonlinear regression.

4. Conclusion

This study successfully demonstrates the green synthesis of crystalline silver nanoparticles (AgNPs) using *Agave americana* leaf extract as a dual reducing and stabilizing agent. Comprehensive characterization confirmed the formation of monodisperse, face-centered cubic (FCC) AgNPs with an average size of 45 ± 12 nm (FESEM) and characteristic surface plasmon resonance at 434 nm (UV-Vis). Thermal analysis revealed exceptional material purity and stability; DSC showed a sharp endothermic peak at 103.88°C (melting point) with no phase transitions up to 350°C (Fig. 9 a), while TGA indicated complete decomposition of organic capping agents by 180°C, confirming protein/polysaccharide-mediated stabilization.

The biosynthesized AgNPs exhibited multifunctional bioactivity: potent antimicrobial efficacy against drug-resistant pathogens, with a notably low MIC of 3.0 µg/mL for *P. aeruginosa* and inhibition zones of 14.5 mm for *P. aeruginosa*, 13.5 mm for *E. coli*, and 16.7 mm for *S. aureus* at 100 µg/mL, compared to gentamicin controls; dose-dependent antioxidant capacity (84.2% DPPH scavenging at 100 µg/mL), though less efficient than ascorbic acid; and selective cytotoxicity against SiHa cervical cancer cells (IC_{50} = 15 µg/mL) mediated by ROS generation.

These findings establish *Agave americana*-derived AgNPs as promising degradable therapeutic carriers, where thermal stability (<350°C) enables biomedical formulation and antioxidant-prooxidant duality explains context-dependent bioactivity. Future research may investigate scalable synthesis protocols for industrial translation, In vivo validation of antitumor efficacy, and surface engineering to optimize antioxidant specificity. The compelling bioactivity demonstrated in this study positions our *Agave americana*-AgNPs at the forefront of green nanotechnology for biomedical applications, a field that is rapidly advancing towards clinical translation.

Author contribution

Abhishek Prakash Tiwari: Conceptualization, Methodology, Formal Analysis, Investigation, Data Curation, Software, Writing- Original draft preparation, **Deepankar Yadav**: Writing – Review & Editing, Investigation, Visualization, Formal Analysis, **Rajkamal Tiwari**: Review & Editing, Investigation, Visualization, Formal Analysis, and **Prof. B. C.**

Yadav: Conceptualization, Resources, Supervision, Validation, and Administration.

Acknowledgement
The authors gratefully acknowledge Babasaheb Bhimrao Ambedkar University (BBAU), Lucknow, for providing institutional support and research facilities. They also thank the Centre of Excellence Programme, Higher Education, Government of Uttar Pradesh, for access to the cell culture facility at the Molecular and Human Genetics Laboratory, Department of Zoology, University of Lucknow.

Conflict of interest
The authors have disclosed no conflicts of interest**.**

References

Aisida, S.O., Ugwu, K., Akpa, P.A., Nwanya, A.C., Nwankwo, U., Botha, S., Ejikeme, P.M., Ahmad, I., Ezema, F.I., 2019. Biosynthesis of silver nanoparticles using bitter leave (*Veronica amygdalina*) for antibacterial activities. Surf. Interfaces 17, 100359.

Alabdallah, N.M., Hasan, M.M., 2021. Plant-based green synthesis of silver nanoparticles and its effective role in abiotic stress tolerance in crop plants. Saudi J. Biol. Sci. 28 (10), 5631-5639.

Alves, M.F., de Oliveira, S.F., Rasbold, L.M., Corrêa, B.O., Ricci-Júnior, E., Santos-Oliveira, R., 2021. *Agave americana* L. extract mediated green synthesis of silver nanoparticles: characterization and biological applications. Mater. Chem. Phys. 267, 124588.

Anjum, S., Abbasi, B.H., Shinwari, Z.K., 2016. Plant-mediated green synthesis of silver nanoparticles using *Agave americana* sucrose-induced callus cultures and their biomedical applications. Ind. Crops Prod. 94, 212-221.

Awwad, A.M., Salem, N.M., Abdeen, A.O., 2013. Green synthesis of silver nanoparticles using *Agave americana* leaf extract: characterization and antibacterial activity. Int. J. Ind. Chem. 4 (29), 1-6.

Brum, L.F., da Silva, M.D., dos Santos, C., Pavoski, G., Espinosa, D.C., da Silva, W.L., 2025. Green synthesis of niobium (V) oxide nanoparticles using pecan nutshell (*Carya illinoinensis*) and evaluation of its antioxidant activity. Catal. Today 445, 115106.

Chamakuri, S.R., Suttee, A., Mondal, P., 2020. An eye-catching and comprehensive review on *Xanthium strumarium* jacq. (bridal bouquet). Plant Arch. 20 (2), 2076-2079.

Chugh, H., Sood, D., Chandra, I., Tomar, V., Dhawan, G., Chandra, R., 2018. Role of gold and silver nanoparticles in cancer nano-medicine. Artif. Cells Nanomed. Biotechnol. 46 (sup1), 1210-1220.

de Menezes, L.B., Druzian, D.M., Oviedo, L.R., Bonazza, G.K., Machado, A.K., da Silva, W.L., 2024. In vitro safety profile and phyto-ecotoxicity assessment of the eco-friendly calcium oxide nanoparticles. Chemosphere 365, 143407.

Dhumale, V.A., Gangwar, R.K., Pande, N., 2021. Importance of gold nanoparticles for detection of toxic heavy metal ions and vital role in biomedical applications. Mater. Res. Innov. 25 (6), 354-360.

Dongsar, T.T., Dongsar, T.S., Gupta, N., Almalki, W.H., Sahebkar, A., Kesharwani, P., 2023. Emerging potential of 5-fluorouracil-loaded chitosan nanoparticles in cancer therapy. J. Drug Deliv. Sci. Technol. 82, 104371.

El-Sonbaty, S.M., 2013. Fungus-mediated synthesis of silver nanoparticles and evaluation of antitumor activity. Cancer Nanotechnol. 4, 73–79.

Elumalai, E.K., Prasad, T.N.V.K.V., Hemachandran, J., Therasa, S.V., Thirumalai, T., David, E., 2010. Extracellular synthesis of silver nanoparticles using leaves of Euphorbia hirta and their antibacterial activities. J. Pharm. Sci. Res. 2 (9), 549-554.

Govindasamy, R., Xuan, J., Sivaraj, C., Arumugam, P., Senthilkumar, S.R., 2020. Synergistic antibacterial and in vitro anticancer efficacy of green synthesized silver nanoparticles using marine macroalgae Sargassum muticum. J. Mol. Struct. 1221, 128828.

Gupta, A., Mumtaz, S., Li, C.H., Hussain, I., Rotello, V.M., 2019. Combatting antibiotic-resistant bacteria using nanomaterials. Chem. Soc. Rev. 48 (2), 315-328.

Iravani, S., 2011. Green synthesis of metal nanoparticles using plants. Green Chem. 13 (10), 2638–2650.

Jain, S., Mehata, M.S., 2017. Medicinal plant mediated synthesis of silver nanoparticles and their antibacterial, anticancer and antioxidant properties. J. Pharm. Anal. 7 (3), 165-172.

Johnsona, P., Krishnana, V., Loganathana, C., Govindhan, K., Raji, V., Sakayanathan, P., Vijayan, S., Sathishkumar, P., Palvannan, T., 2018. Rapid biosynthesis of Bauhinia variegata flower extract-mediated silver nanoparticles: an effective antioxidant scavenger and α-amylase inhibitor. Artif. Cells Nanomed. Biotechnol. 46 (7), 1488–1494.

Jyoti, K., Singh, A., Fekete, G., Singh, T., 2020. Cytotoxic and radiosensitizing potential of silver nanoparticles against HepG-2 cells prepared by biosynthetic route using Picrasmaquassioides leaf extract. J. Drug Deliv. Sci. Technol. 55, 101479.

Khatami, M., Sharifi, I., Nobre, M.A., Zaeifi, A., Pourseyedi, S., 2016. Waste-to-nanomaterial: Biogenic synthesis of silver nanoparticles using orange peel extract, characterization, and bioactivity. J. Mol. Liq. 218, 417-422.

Khan, I., Saeed, K., Khan, I., 2019. Nanoparticles: properties, applications and toxicities. Arab. J. Chem. 12 (7), 908-931.

Mason, C., Vivekanandhan, S., Misra, M., Mohanty, A.K., 2012. Switchgrass (Panicum virgatum) extract mediated green synthesis of silver nanoparticles. World J. Nano Sci. Eng. 2 (2), 47–52.

Mukherjee, P., Ahmad, A., Mandal, D., Senapati, S., Sainkar, S.R., Khan, M.I., Parishcha, R., Ajaykumar, P.V., Alam, M., Kumar, R., 2001. Fungus-mediated synthesis of silver nanoparticles and their immobilization in the mycelial matrix: a novel biological approach to nanoparticle synthesis. Nano Lett. 1 (10), 515–519.

Mukhopadhyay, D., Dasgupta, P., Roy, D.S., Palchoudhuri, S., Chatterjee, I., Ali, S., Dastidar, S.G., 2016. A sensitive in vitro spectrophotometric hydrogen peroxide scavenging assay using 1, 10-phenanthroline. Free Radic. Antioxid. 6 (1), 124-132.

Muniz, F.T.L., Miranda, M.A.R., Santos, C.M.D., Sasaki, J.M., 2016. The Scherrer equation and the dynamical theory of X-ray diffraction. Acta Crystallogr. Sect. A: Found. Adv. 72 (3), 385–390.

Muraro, P.C., Wouters, R.D., Druzian, D.M., Viana, A.R., Schuch, A.P., Rech, V.C., Da Silva, W.L., 2024. Ecotoxicity and in vitro safety profile of the eco-friendly silver and titanium dioxide nanoparticles. Process Saf. Environ. Prot. 188, 584-594.

Parveen, S., Kumar, S., Pal, S., Yadav, N.P., Rajawat, J., Banerjee, M., 2023. Enhanced therapeutic efficacy of Piperlongumine for cancer treatment using nano-liposomes mediated delivery. Int. J. Pharm. 643, 123212.

Pompeu, L.D., Viana, A.R., da Silva Fernandes, L., da Silva, W.L., 2023. Evaluation of cytotoxicity, reactive oxygen species and nitrous oxide of nanochitosan from shrimp shell. Int. J. Biol. Macromol. 235, 123730.

Raj, L.F.A.A., Jayalakshmy, E., 2015. Biosynthesis and characterization of zinc oxide nanoparticles using root extract of Zingiber officinale. Orient. J. Chem. 31 (1), 51–56.

Ramanery, F.P., Mansur, A.A., Mansur, H.S., 2014. One-step green synthesis of silver nanoparticles using carboxymethylcellulose as reducing agent and stabilizer for killing HeLa cervical cancer cells. Carbohydr. Polym. 111, 804-814.

Rana, A., Yadav, K., Jaggi, S., 2020. Green synthesis of silver nanoparticles using plant extract and their antibacterial and antifungal activities. J. Microbiol. Biotechnol. Res. 10 (2), 14-22.

Ravilla, L.E., Lavanya, M., Padmini, R., 2023. Sustained anticancer effect by naringin-loaded zinc oxide nanoparticles in human lung adenocarcinoma A549 cells. Int. J. Appl. Pharm. 15, 315-325.

Ravichandran, D., Megala, M.A., Anbalagan, K., Srivastava, P., Al-Dosary, M.A., Hatamleh, A.A., Murugesan, S., 2025.Eco-friendly synthesis of biochar-CoFe2O4 nanocomposites using Ulva lactuca L. for photocatalytic degradation of Congo red and in vitro biological applications. Colloids Surf. A: Physicochem. Eng. Aspects 713, 136465.

Ravichandran, N., Uvarajan, D., Ravikumar, M., Mahendhran, K., Krishnamoorthy, K., Vellingiri, B., Govindasamy, C., Narayanasamy, A., 2025. Gracilaria edulis-mediated silver nanoparticles as a targeted strategy for cervical cancer with integrated toxicity evaluation in zebrafish. Bioorg. Chem. 108361.

Salayová, A., Bedlovičová, Z., Daneu, N., Baláž, M., Lukáčová Bujňáková, Z., Balážová, Ľ., Tkáčiková, Ľ., 2023. Green synthesis of silver nanoparticles using *Agave americana* L. leaf extract: characterization, antibacterial activity, and cytotoxicity. Heliyon 9 (3), 13876.

Sathishkumar, M., Sneha, K., Won, S.W., Cho, C.W., Kim, S., Yun, Y.S., 2009. *Cinnamon zeylanicum* bark extract and powder mediated green synthesis of nano-crystalline silver particles and its bactericidal activity. Colloids Surf. B: Biointerfaces 73 (2), 332-338.

Shereen, M.A., Ahmad, A., Khan, H., Satti, S.M., Kazmi, A., Bashir, N., Shehroz, M., Hussain, S., Ilyas, M., Khan, M.I., 2024. Plant extract preparation and green synthesis of silver nanoparticles using Swertia chirata: Characterization and antimicrobial activity against selected human pathogens. Heliyon 10 (10), e28038

Cite this article:
Tiwari, A. P., Yadav, D., Tiwari, R., Yadav, B.C.,2026. Bio-fabricated *Agave americana* Silver Nanoparticles: Dual Antimicrobial–Anticancer Efficacy Rooted in Structural and Thermal Characteristics
J. Appl. Sci. Innov. Technol. 5 (1), 32-39.